Planet. Space Sci. Vol. 29, No. 10, pp. 1095–1099, 1981.
Printed in Great Britain.

0032–0633/81/101095–05$02.00/0

NON-THERMAL O(^{1}D) PRODUCED BY DISSOCIATIVE RECOMBINATION OF O_2^+: A THEORETICAL MODEL AND OBSERVATIONAL RESULTS

G. A. SCHMITT, V. J. ABREU and P. B. HAYS
Space Physics Research Laboratory, The University of Michigan, Department of Atmospheric and Oceanic Science, Ann Arbor, MI 48109, U.S.A.

(*Received* 5 *June* 1981)

Abstract—Thermal and non-thermal O(^{1}D) number density profiles are calculated. The two populations are assumed to be coupled by a thermalization cross-section which determines the loss and production in the non-thermal and thermal populations, respectively. The sources, sinks and transport of the two populations are used to model volume emission rate profiles at 6300 Å. The 6300 Å brightness measured by the Visible Airglow Experiment is then used to establish the presence of the non-thermal population and to determine the thermalization cross-section.

INTRODUCTION

The presence of a non-thermal population of atomic oxygen in the thermosphere has been the subject of many theoretical studies over the years (Hays and Walker, 1966; Torr *et al.*, 1974; Shizgal and Lindenfeld, 1979; Torr *et al.*, 1979a; Yee and Hays, 1980). Several attempts have been made to detect non-thermal oxygen atoms from ground-based optical observations. An attempt made by Biondi and Feibelman (1978) to detect the O(^{1}D) 6300 Å emission signature profile in the nightglow resulted inconclusive. Hernandez (1971) first successfully detected the non-Maxwellian signature of the O(^{1}S) 5577 Å airglow emission near the magnetic equator. More recently, Yee *et al.* (1980) have experimentally shown that above 500 km during the maximum of the solar cycle the atomic oxygen density is enhanced beyond the level determined by a model atmosphere calculated on the assumption of thermal equilibrium. Yee's technique involved measuring the 7320–30 Å [($O^+(^2P)$–$O^+(^2D)$)] airglow emission at twilight.

At night, the main source of O(^{1}D) atoms is the dissociative recombination of O_2^+ (Hays *et al.*, 1978) formed by

$$O^+ + O_2 \rightarrow O_2^+ + O.$$

The reaction

$$O_2^+ + e \rightarrow O(^1D) + O(^3P, {}^1D \text{ or } {}^1S)$$

is exothermic with a net excess energy of 6.98 eV per recombination. This energy must be conserved either as excitation energy in the product atoms or as kinetic energy. The amount of kinetic energy depends on the electronic state (^{3}P, ^{1}D or ^{1}S) of the product oxygen atoms.

The fate of O(^{1}D) atoms with suprathermal kinetic energies depends on the nature of the interactions following their creation. The simplest models used to approximate observed red line (6300 Å) properties assume the O(^{1}D) population to have a thermal velocity distribution. This is a good approximation at low altitudes, where collision frequencies are high and departures from local thermal equilibrium are strongly damped. At high altitudes, however, the relaxation toward a thermal distribution is relatively slow and non-thermal velocity distributions are likely.

This study will consider the 6300 Å emission of a two-population O(^{1}D) model first developed by Hays and Walker (1966). The model consists of one subpopulation which is non-thermal and arises from the dissociative recombination of O_2^+. Sinks for the subpopulation include collisional quenching, emission of radiation (6300 Å) and 'thermalization' by O(^{3}P). The second subpopulation is thermally distributed and consists of O(^{1}D) atoms thermalized by the O(^{3}P). Sinks for the thermal subpopulation include collisional quenching and radiation. The two populations are thus coupled by a 'thermalization cross-section' which determines the loss and production in the non-thermal and thermal populations, respectively. The sources, sinks and transport of the two populations just mentioned will be used in this paper to model volume emission rate profiles of the O(^{1}D) emission at 6300 Å. The 6300 Å brightness measured by the Visible Airglow Experiment (Hays *et al.*, 1973) will be used to establish the presence of a non-thermal population and to determine the 'thermalization cross-section'.

THEORY

The two-population model of Hays and Walker (1966) has been adapted to calculate altitude profiles of thermal and non-thermal $O(^1D)$ densities. The model assumes that non-thermal $O(^1D)$ atoms, created by the dissociative recombination of O_2^+, are thermalized by single collisions with thermal $O(^3P)$ atoms. The probability that fast product atoms created at altitude Z_0 and zenith angle ϕ will be neither quenched nor thermalized at altitude Z is given by

$$S(Z, Z_0) = \exp\left[-\tau(Z, Z_0)/\mu\right], \quad (1)$$

where

$$\tau(Z, Z_0) = \sigma_0 N_0(Z, Z_0) + \sigma_Q N_{N_2}(Z, Z_0) + \frac{A_{^1D}(Z - Z_0)}{|\mathbf{V}|}, \quad (2)$$

$$N_i(Z, Z_0) = \int_Z^{Z_0} n_i(Z')\,dZ', \quad (3)$$

- μ $\cos\phi$
- n_i number density of the ith species
- σ_0 thermalization cross-section
- σ_Q cross-section for quenching
- $A_{^1D}$ spontaneous emission rate for $O(^1D)$ atoms
- $\mathbf{V}$ velocity of the product oxygen atom.

The fate of a non-thermal $O(^1D)$ atom is represented in equation (2) by three terms which include the probabilities of quenching by N_2, spontaneous radiation at 6300 Å, and thermalization in one collision by excitation exchange with $O(^3P)$. We note that gravitational effects on the non-thermal atoms are ignored.

The flux of non-thermal $O(^1D)$ atoms at Z due to production in a layer between Z_0 and $Z_0 + dZ_0$ is

$$P'(Z, Z_0)\,dZ_0 = \int_0^1 \frac{P(Z_0)}{2\mu} e^{-\tau/\mu}\,dZ_0\,d\mu, \quad (4)$$

where

$$P(Z_0) = \beta_{^1D}[O_2^+]n_e = 1.33K_1[O_2]Fn_e, \quad (5)$$

and

$$F = 1/\{1 + K_1[O_2]/\beta_1 n_e + K_2[N_2]/\beta_2 n_e\}.$$

- n_e electron number density
- $[O_2^+]$ molecular oxygen ion number density
- $[O_2]$ molecular oxygen number density
- $[N_2]$ molecular nitrogen number density
- K_1 rate constant for the production of O_2^+
- K_2 rate constant for the production of NO^+
- β_1 rate constant for the dissociative recombination of O_2^+
- β_2 rate constant for the dissociative recombination of NO^+
- $\beta_{^1D}$ specific recombination rate for the production of $O(^1D)$.

The rate of production of $O(^1D)$ atoms by the dissociative recombination of O_2^+ is given in equation (5).

The 6300 Å emission rate of the non-thermal $O(^1D)$ population is

$$\eta_{NT}(Z) = \frac{A_{^1D}}{2|\mathbf{V}|}\int_0^\infty P'(Z, Z_0)\,dZ_0 = \frac{A_{^1D}}{2|\mathbf{V}|}\int_0^\infty P(Z_0)E_1(\tau)\,dZ_0, \quad (6)$$

where

$$E_1(\tau) = \int_\tau^\infty \frac{e^{-x}}{x}\,dx. \quad (7)$$

Equation (7) is the integral over all zenith angles of the probability that an atom created at altitude Z_0 will reach Z.

The altitude profile of the thermalized $O(^1D)$ number density is calculated by solving the one-dimensional continuity equation for a minor constituent diffusing through a stationary atmosphere. The one-dimensional continuity equation is

$$\frac{\partial}{\partial Z}\left\{D(Z)\left[\frac{\partial N(Z)}{\partial Z} + N(Z)\left(\frac{\partial \ln T(Z)}{\partial Z} + \frac{1}{H(Z)}\right)\right]\right\} = P'(Z) - L(Z)N(Z), \quad (8)$$

where

$$P'(Z) = \frac{\sigma_0 N_0(Z)}{2}\int_0^\infty P(Z_0)E_1(\tau)\,dZ_0 \quad (9)$$

$$L(Z)N(Z) = (A_{^1D} + K_Q[N_2(Z)])N(Z). \quad (10)$$

- $D(Z)$ Diffusion coefficient
- $H(Z)$ scale height of thermal $O(^1D)$
- $N(Z)$ thermal $O(^1D)$ number density
- K_Q rate constant for quenching of thermalized $O(^1D)$.

The production rate of the thermal component is determined by the thermalization rate of the non-thermal population, as shown in equation (9). The loss processes of thermalized O(^{1}D) are described in equation (10) by two terms representing destruction by spontaneous radiation and quenching by N_2, respectively (Hays *et al.*, 1978). The 6300 Å volume emission rate of thermalized O(^{1}D) atoms is

$$\eta_{th}(Z) = A_{1_D} N(Z). \qquad (11)$$

Figure 1 shows the two components of an O(^{1}D) number density profile obtained by the methods outlined above. The solution to equation (8) was obtained by a finite-difference technique. The MSIS neutral atmosphere model (Hedin *et al.*, 1977a, b) was used for these calculations. The electron density profile used was one obtained at Arecibo on October 26, 1977 at 23:00 h. Other parameters used in the calculation are shown in Table 1. Profiles of the non-thermal component are shown in Fig. 2 for values of σ_0 equal to 0.5×10^{-15}, 1.2×10^{-15} and 2.0×10^{-15} cm^2, respectively. In all cases it was assumed that the dissociative recombination of O_2^+ leads to the formation of one O(^{1}D) atom with an excess energy of 3.1 eV.

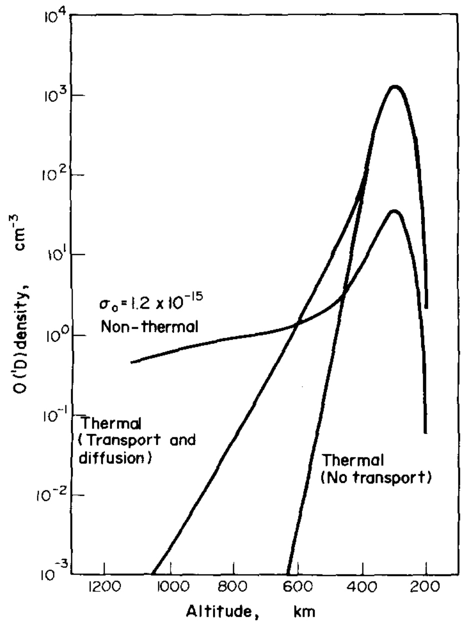

FIG. 1. THERMAL AND NON-THERMAL O(^{1}D) NUMBER DENSITY PROFILES CALCULATED USING THE TWO-POPULATION MODEL. A THERMALIZATION CROSS-SECTION EQUAL TO 1.2×10^{-15} cm^2 WAS USED. THE EFFECT OF TRANSPORT AND DIFFUSION ON THE THERMAL COMPONENT IS SHOWN.

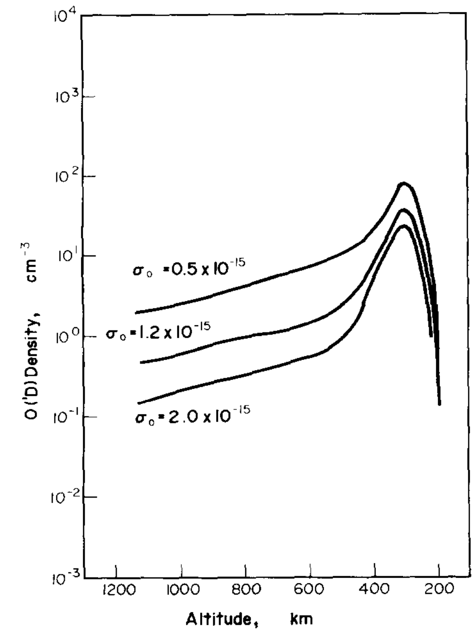

FIG. 2. NON-THERMAL O(^{1}D) NUMBER DENSITY PROFILES CALCULATED USING DIFFERENT THERMALIZATION CROSS-SECTIONS.

THERMALIZATION CROSS-SECTION

The thermalization cross-section will be estimated from the 6300 Å emission measurements made by the Visible Airglow Experiment (VAE) on the Atmosphere Explorer Satellite-C. The VAE instrument has been described by Hays *et al.* (1973). The use of VAE data was based on the expectation that red line emission at high altitudes results entirely from the non-thermal O(^{1}D) population. The model calculations just presented indicate that the expected non-thermal red line intensities at high altitudes are observable and that they are a relatively strong function of the thermalization cross-section. This study has used data obtained by the wide angle channel in the VAE instrument during the spinning mode.

The data selected for analysis in a spin cycle is measured from the vertical direction toward the

TABLE 1.

$\sigma_Q = 1.38 \times 10^{-16}$ cm^2
$A_{1_D} = 0.0068$ s^{-1}
$K_1 = 2 \times 10^{-11} (300/T)^{0.4}$ cm^3 s^{-1}
$\beta_{1_D} = 2.1 \times 10^{-7} (300/T)^{0.55}$ cm^3 cm^{-1}
$K_Q = 2.3 \times 10^{-11}$ cm^3 s^{-1}

Earth's limb. The red line volume emission profile is sampled at high altitudes, where we expect to observe the faint non-thermal emission, and at low altitudes, where the peak of the thermal population emission profile is found. Data have been selected with care that the field of view of the photometer were not illuminated by daylight or auroral emissions. Data have also been selected during geomagnetically quiet times and at midlatitudes. The contributions of extraterrestrial sources (zodical light and galactic background) to the observations are of importance and have been carefully removed. The fact that only elliptical orbits have been chosen for this study allowed the photometer to look at the same region in inertial space during different spin cycles and satellite altitudes. When the satellite was at high altitude, observations at a given angle included only contributions from extraterrestrial sources. As the satellite descended, each observation in the same direction was assumed to include the same contribution from the galaxy plus the red line emission. Extraterrestrial emissions were thus measured and subtracted.

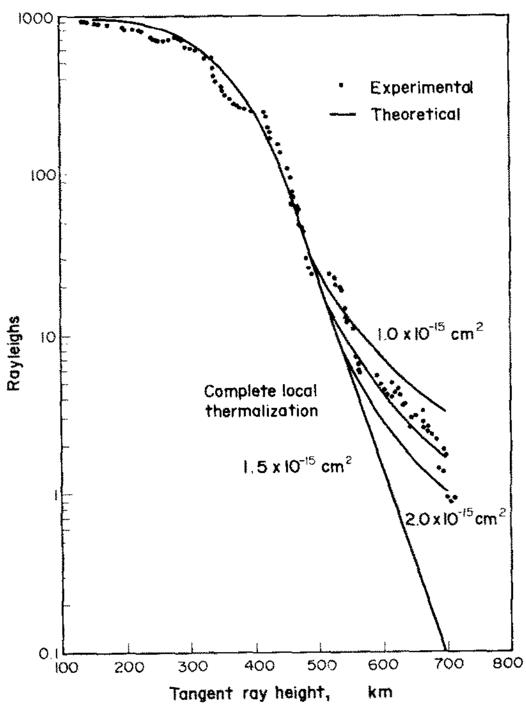

FIG. 3. LIMB SCANS OF THE RED LINE EMISSION MEASURED BY THE VISIBLE AIRGLOW EXPERIMENT. THE ORDINATE IS THE INTEGRATED 6300 Å EMISSION ALONG THE PHOTOMETER LINE OF SIGHT. THE ABSCISSA IS THE TANGENT HEIGHT OF THE LINE OF SIGHT. CALCULATED LIMB SCANS OF THE RED LINE ARE SHOWN FOR THERMALIZATION CROSS-SECTIONS EQUAL TO 1.0, 1.5 and 2.0×10^{-15} cm^2, AND FOR A COMPLETELY THERMALIZED POPULATION.

Figure 3 shows averaged limb scans of the red line emission. The ordinate is the integrated red line emission along the photometer's line of sight. The abscissa is the tangent height of the line of sight. These data have been corrected for the extraterrestrial emission. Data were taken at a satellite altitude ranging from 670 to 820 km, during orbits 1043, 1053 and 1054 of satellite AE–C. The time of the observations is approximately 20.00 h on March, 1974. For comparison purposes the figure also shows the results of a calculation of the limb brightness for thermalization cross sections (cm^2) equal to 1.0, 1.5 and 2.0×10^{-15}, and for a completely thermalized population. The calculated emission levels were derived from a numerical integration along the photometer line of sight of volume emission rates modelled as described in the previous section. A convolution of this brightness was then effected with the VAE instrument function. The geometrical factor due to observations of a tangent height from different spacecraft altitudes was included in the calculation. The shape of the electron density profile used in the calculation was that of a profile obtained at Millstone Hill in March 1973 at 20.00 h. The peak electron density (4.0×10^5 cm^{-3}) was adjusted to match the observed peak brightness. The observed data show the presence of a non-thermal population. The thermalization cross-section is estimated to be within the 1.0–2.0×10^{-15} range.

CONCLUSION

We have shown, by analysis of the VAE data, that the non-thermal red line intensities at high altitudes are observable. A single collision two population $O(^1D)$ model has been presented in which the thermal and non-thermal populations are coupled by a thermalization cross-section. This cross-section has been estimated from a comparison of the observational data with calculated results. A value in the range from 1.0 to 2.0×10^{-15} cm^2 has been assigned to the thermalization cross-section.

Acknowledgment—This work was supported by NASA Grant No. NAS5-23006.

REFERENCES

Biondi, M. A. and Feibelman, W. A. (1968). Twilight and nightglow spectral line shapes of oxygen λ6300 and λ5577 radiation. *Planet. Space Sci.* **16**, 431.

Hays, P. B. and Walker, J. C. G. (1966). Doppler profiles of the 5577 Å airglow. *Planet. Space Sci.* **14**, 1331.

Hays, P. B., Rusch, D. W. Roble, R. G. and Walker, J. C.

G. (1978). The OI(6300 Å) Airglow. *Rev. Geophys. Space Phys.* **16**, 225.

Hays, P. B., Carignan, G. R. Kennedy, B. C. Shepherd, G. G. and Walker, J. C. G. (1973). The visible airglow experiment on Atmosphere Explorer. *Radio Sci.* **8**, 369.

Hedin, A. E., Salah, J. E. Evans, J. V. Rever, C. A. Newton, G. P. Spencer, N. W. Kayser, D. C. Alcayde, D. Bauer, P. Cogger, L. L. and McClure, J. P. (1977a). A global thermospheric model based on mass spectrometer and incoherent scatter data MSIS 1: N_2 density and temperature. *J. geophys. Res.* **82**, 2139.

Hedin, A. E., Reber, C. A. Newton, G. P. Spencer, N. W. Brinton, H. C. and Mayr, H. G. (1977b). A global thermospheric model based on mass spectrometer and incoherent scatter data MSIS 2: Composition. *J. geophys. Res.* **82**, 2148.

Hernandez, G. The signature profiles of O(^{1}S) in the airglow. *Planet. Space Sci.* **19**, 467.

Shizgal, B. and Lindenfeld, M. J. (1979). Energy distribution ^{3}P function of translationally hot O(^{3}P) atoms in the atmosphere of the earth. *Planet. Space Sci.* **27**, 1321.

Torr, M. R., Walker, J. C. G. and Torr, D. G. (1974). Escape of fast oxygen from the atmosphere during geomagnetic storms. *J. geophys. Res.* **79**, 5267.

Torr, M. R. and Torr, D. G. (1979). Energetic oxygen. A direct coupling mechanism between the magnetosphere and thermosphere. *Geophys. Res. Lett.* **6**, 700.

Yee, J. H. and Hays, P. B. (1980). The oxygen polar corona. *J. geophys. Res.* **75**, 1795.

Yee, J. H., Meriwether, J. W. Jr. and Hays, P. B. (1980). Detection of a corona of fast oxygen atoms during solar maximum. *J. geophys. Res.* **85**, 3396.